Fusion Engineering and Design 208 (2024) 114703

Contents lists available at ScienceDirect

Fusion Engineering and Design

journal homepage: www.elsevier.com/locate/fusengdes

Numerical investigation of the structural performances of the EU-DEMO Water-Cooled Lead Lithium breeding blanket equipped with helicoidal double-walled tubes

J.A. Noguerón [a], P.A. Di Maio [b], G. Bongiovì [b,*], I. Catanzaro [b], P. Chiovaro [b], S. Giambrone [b], A. Quartararo [b], E. Vallone [b], I. Fernández-Berceruelo [a], P. Arena [c]

[a] CIEMAT, National Fusion Laboratory, Avda. Complutense 40, 28040 Madrid, Spain
[b] Department of Engineering, University of Palermo, Viale delle Scienze, Ed. 6, 90128 Palermo, Italy
[c] Nuclear Department, ENEA C. R. Brasimone, 40032 Camugnano Bologna, Italy

ARTICLE INFO

Keywords:
DEMO WCLL
Breeding blanket
Thermo-mechanics
FEM analysis
Helicoidal tubes

ABSTRACT

With the aim of improving the EU-DEMO breeding blanket (BB) system performances, variants to the reference design are presently under investigation in the EUROfusion activities. Among them, a novel layout for the double-walled tubes (DWTs) aimed at cooling the breeding zone is being studied for the Water-Cooled Lead Lithium (WCLL) BB concept. The new DWTs configuration consists of 6 couples of helical-shaped DWTs, with each tubes couple being positioned in a slot defined by the radial-poloidal stiffening plates (SPs). The adoption of the helicoidal tubes layout shall allow reducing the thermal hotspots in the BB structural material, being beneficial also in terms of thermal stress. Hence, a structural analysis of the equatorial region of the WCLL BB central outboard blanket segment has been performed and presented in this work.

The structural assessment has been conducted under various loading scenarios, including Normal Operation (NO), with nominal and design pressure values, and NO scenario considering buoyancy effects induced by the liquid breeder. All these scenarios assumed the same previously obtained thermal field to predict displacements and stress fields. Subsequently, a stress linearization procedure has been performed in some critical regions of the structure, which allows comparing the stress values obtained with the criteria prescribed by the reference design standard RCC-MRx. The outcomes derived from this evaluation, in terms of stresses and displacements, seem very promising. However, some contact regions have been identified in the tubes, necessitating careful consideration of geometric modifications in future analyses. Nevertheless, the obtained results clearly show that the proposed layout is worthy to be further assessed. A theoretical–numerical approach based on the Finite Element Method (FEM) was followed adopting the Ansys commercial code.

1. Introduction

On the road to achieve electricity production by nuclear fusion at commercial level, the DEMOnstration reactor (DEMO) is postulated to be the first device that shall demonstrate the integrated operation of technologies necessary for net power. Within this context, the Breeding Blanket (BB) is probably the most critical in-vessel system in charge of multiplication and extraction of power, tritium production through Li^6 (n, α) H^3 reactions, and radiation shielding. Operating inside a nuclear fusion reactor, the BB must withstand a range of extreme conditions (high heat flux, temperatures, neutron damage, electromagnetic forces, etc.). In the last decades, under the umbrella of the EUROfusion consortium, research activities have been focused on different BB concept designs that contemplate different coolants, breeders and neutron multiplier materials. They have concluded in the selection of two possible BB design candidates to be used as driver blanket of the EU-DEMO fusion reactor [1]: the Helium-Cooled Pebble Bed (HCPB) [2] and the Water-Cooled Lead-Lithium (WCLL) [3].

The current WCLL BB design follows a Single Module Segment (SMS) architecture [4-6] that relies on Eurofer as the structural material [7]. Pressurized water at 15.5 MPa is used as the coolant, operating within a temperature range of 295–328 °C [3,4], so as to operate in the

* Corresponding author.
E-mail address: gaetano.bongiovi@unipa.it (G. Bongiovì).

https://doi.org/10.1016/j.fusengdes.2024.114703
Received 24 July 2024; Received in revised form 23 October 2024; Accepted 24 October 2024

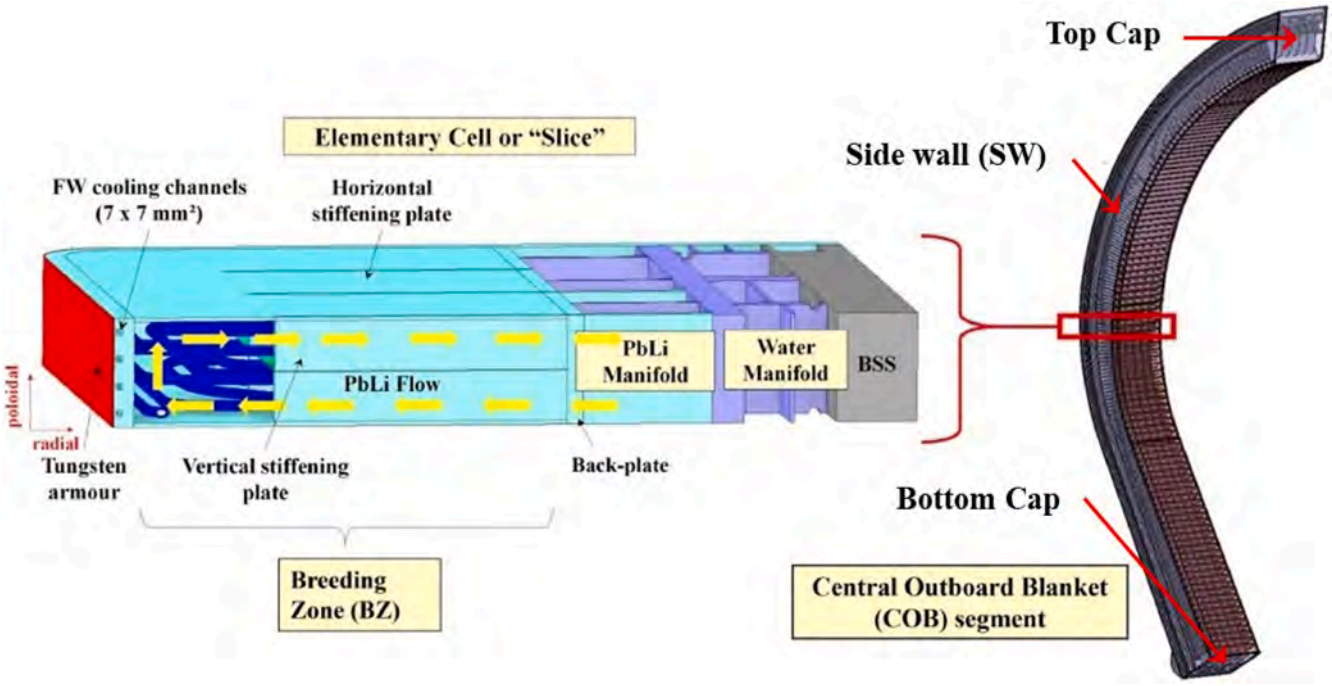

Fig. 1. Design of WCLL COB segment and reference elementary cell [10].

thermodynamic conditions typical of the worldwide deployed fission Pressurized Water Reactors (PWRs). A PbLi eutectic liquid alloy [8] serves multiple roles: it acts as a neutron multiplier (due to lead), a tritium breeder (with lithium enriched to 90 % in Li^6), an energy multiplication medium (since neutron multiplication and tritium breeding reactions are exoergic) and a tritium carrier, transporting tritium to the Tritium Extraction and Removal (TER) system [3,4].

Despite the advanced design and proven cooling performance of the current Double-Walled Tubes (DWTs) C-shaped layout, several limiting factors need to be addressed to enhance the maturity of the WCLL BB design [9]. One of the most crucial issues is the need to reduce the water mass in the breeding zone (BZ) for neutronic purposes, without compromising the cooling performance of the DWTs. Another main concern is the elevated number of DWTs in the current BB configuration that endangers the reliability of the system because of the extensive number of welds required. Other potential improvements concern the possibility of having a more standardized DWTs design, a simpler BB manufacturability and a simpler flow distribution in the manifold avoiding the water recirculation, currently envisaged for the reference DWTs architecture. Consequently, the introduction of helical-shaped DWTs in the WCLL BB architecture is being considered and is currently under investigation [10].

Thermal-hydraulic and neutronic analyses performed in the WCLL Central Outboard Blanket (COB) segment equatorial region equipped with helical-shaped tubes demonstrated the promising performance of this design under nominal loading conditions. In particular, the studies indicate that the cooling layout can withstand the imposed heat loads and meet the DEMO design requirements, ensuring an adequate temperature field within the Eurofer stiffening plates (SPs), baffle plates, and first wall (FW). Indeed, the temperature limit of 550 °C is not reached in the solid structures [10]. Hence, in the present work, the investigation of the structural behaviour of the WCLL COB segment equatorial region equipped with helical-shaped tubes is described, in order to complete the assessment of the potentialities of this alternative DWTs design concept. To this purpose, a numerical approach based on the Finite Element Method (FEM) has been followed by the adoption of the quoted commercial Ansys code.

2. The WCLL COB segment with helical-shaped tubes

In this section, the overall WCLL BB geometric layout and the two variants of cooling tubes currently under consideration are presented and critically discussed.

2.1. General WCLL BB layout

The current EU-DEMO configuration [11] divides the reactor into 16 sectors of 22.5° each, defined by its toroidal field coils. The WCLL BB layout follows this segmentation, with each sector further divided into five BB segments: two in the inboard region (Left and Right) and three in the outboard region (Left, Central and Right). Fig. 1 provides the general layout of the WCLL COB segment. It is also shown the reference elementary cell, which is the portion of the segment that is repetitive along the poloidal direction. Each segment is well characterized by the integration of the following components:

- FW, consists of a continuous U-shaped panel of 25 mm, which is actively cooled by pressurized water. It is covered by a 2 mm tungsten layer that is used as plasma-facing material.
- The breeding zone (BZ), this region, embedded into the FW structure, contains the PbLi eutectic alloy, which serves as tritium production and neutron multiplication. The structure is reinforced with a grid of radial-toroidal and radial-poloidal SPs (10 and 12 mm thick respectively). Additionally, a set of horizontal baffle plates (2 mm thick), located in the poloidal-mid planes are used to direct the breeder flow along its path in the BZ, having no structural function. This region, subjected to the highest nuclear heating (NH) conditions, is cooled by pressurized water DWTs.
- Manifolds region, where the PbLi and water are distributed and collected.
- Back Supporting Structure (BSS), a structure to withstand the mechanical loads and connect the BB with the Vacuum Vessel (VV).
- Caps, plates actively cooled to close the BB segment in the poloidal directions.

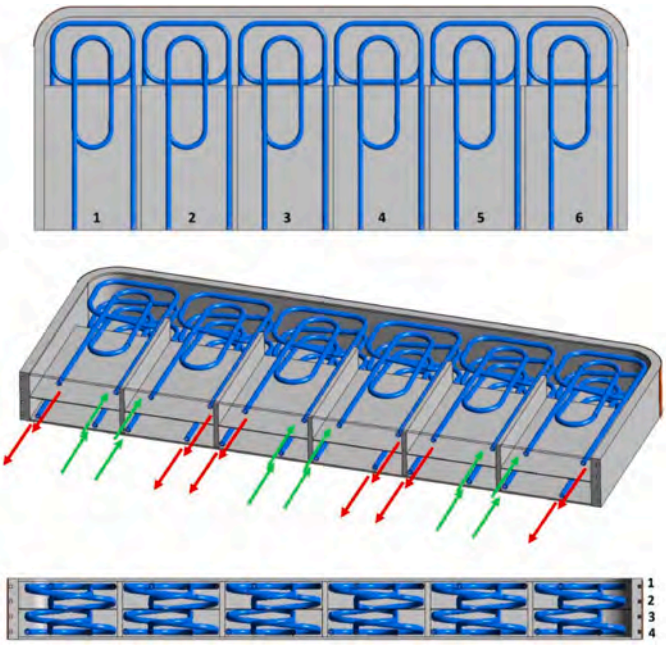

Fig. 2. Helical-shaped DWT layout of the WCLL BB slice (arrows represent coolant inlet and outlet directions) [10].

2.2. Comparison of DWTs layout

In the current design of the WCLL BB for the EU-DEMO reactor, the cooling system employs DWTs with a C-shaped configuration [3,12]. It adopts pressurized water (15.5 MPa, 295–328 °C) to cool the structural components and the PbLi eutectic alloy [8]. This layout ensures efficient heat removal and maintains the operational integrity of the BB structure under high heat flux conditions. However, despite its maturity and proven performance, the current DWTs configuration presents several challenges that need to be addressed to improve the overall design's maturity.

One limitation of the C-shaped configuration is the high number of welds, due to the extensive number of DWTs, which can impact the system's reliability [9]. The welds are potential points of failure, and their high quantity increases the complexity of manufacturing and maintenance. Additionally, for neutronic purposes, there is a need to minimize the water mass in BZ without compromising the cooling performance. This reduction is necessary to enhance the tritium breeding efficiency and overall reactor performance. Moreover, the current configuration's complexity calls for improvements in the DWT design standardization, manufacturability, and fluid flow distribution to avoid water recirculation issues currently present in the reference DWT architecture [3,12,13].

The proposed solution involves replacing the C-shaped DWTs with helical-shaped DWTs (Fig. 2) [10]. This new layout is designed to address the existing issues by leveraging the unique advantages of the helical shape. The tubes helical configuration offers several benefits:

- Enhanced Cooling Performance: the helical tubes facilitate better heat transfer and coolant flow dynamics, leading to more efficient cooling of the BZ.
- Increased Tritium Breeding Ratio (TBR): by optimizing the spatial arrangement and cooling efficiency, the helical tubes can contribute to a higher TBR, crucial for sustaining the fusion reaction.
- Simplified Cooling Water Flow-Path: the helical layout can streamline the coolant flow path, reducing complexity and potential bottlenecks such as water recirculation, thereby improving the overall efficiency of the cooling system.

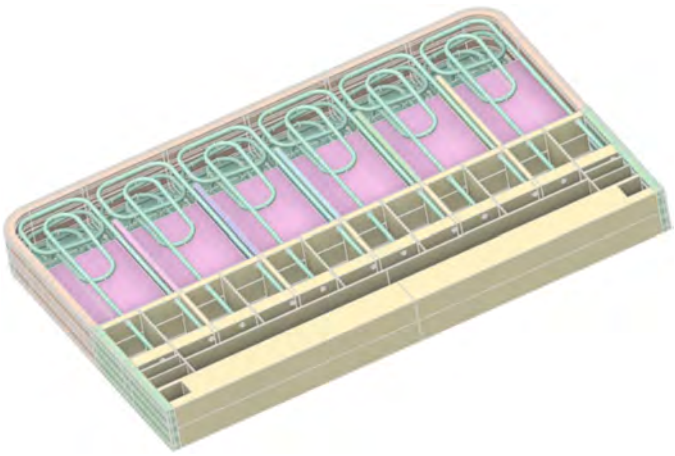

Fig. 3. Elementary cell of the helical-shaped WCLL BB.

- Improved reliability: by a reduction of the DWTs number with respect to the C-shape layout, and therefore, reducing the number of welds required in each cell. However, the manufacturing on one single tube will be more challenging.

Computational Fluid Dynamics (CFD) analyses have been conducted to evaluate the thermal-hydraulic performance of the helical-shaped DWTs. The results indicate that the new layout significantly outperforms the existing C-shaped configuration in terms of thermal management. The helical configuration ensures better heat dissipation, maintaining adequate temperature control within critical components such as the Eurofer stiffeners, baffle plates, and the FW. This improved cooling performance ensures that the temperature limit of 550 °C is not reached in the solid structures, thereby preserving the structural integrity and operational safety of the blanket [10].

Neutronic studies indicate a slight increase in the TBR has been achieved in comparison with the C-shaped configuration. This improvement is produced due to the optimization of the coolant flow path, which allows a reduction of the water mass and therefore increasing the breeder volume [10]. Nevertheless, further investigations must be performed to achieve the design target for tritium self-sufficiency of 1.15 [14].

In summary, the helical-shaped DWTs present a substantial improvement over the current C-shaped design. They offer enhanced reliability, better cooling performance, a higher TBR, and a more straightforward coolant flow path. These improvements are expected to contribute significantly to the WCLL BB's overall efficiency and effectiveness, making it a more viable and robust solution for the EU-DEMO fusion reactor.

3. FEM models

In this section, the FEM models set-up for the structural analysis of the WCLL COB equatorial region equipped with helical-shaped tubes are described, adequately motivating the adopted assumptions.

3.1. Geometrical considerations

To perform the structural analysis, the same geometric model already adopted for the thermal-hydraulic and neutronic studies has been used [10]. It represents the elementary cell (Fig. 3) of the WCLL COB segment equatorial region, encompassing the proper portion of the tungsten layer, the First Wall-Side Walls (FW-SWs) actively cooled by means of 4 poloidally distributed channels, the horizontal and vertical stiffening plates, one baffle plate and the 12 helical-shaped DWTs [10].

To adequately conduct structural analysis, the elementary geometric

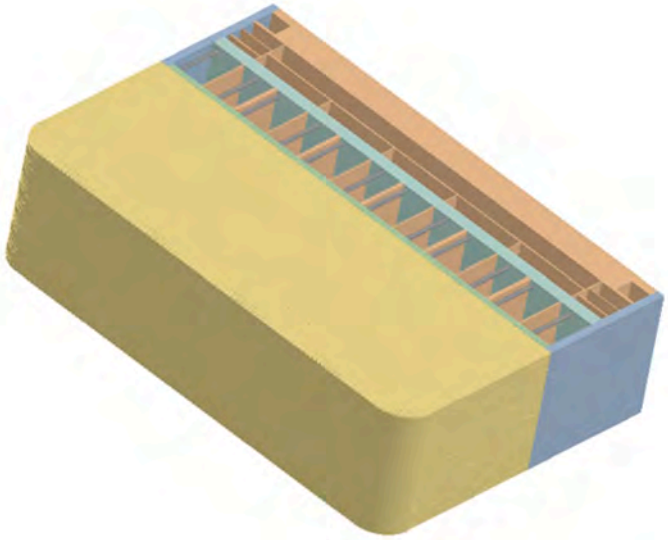

Fig. 4. Geometrical model with duplication of the slices.

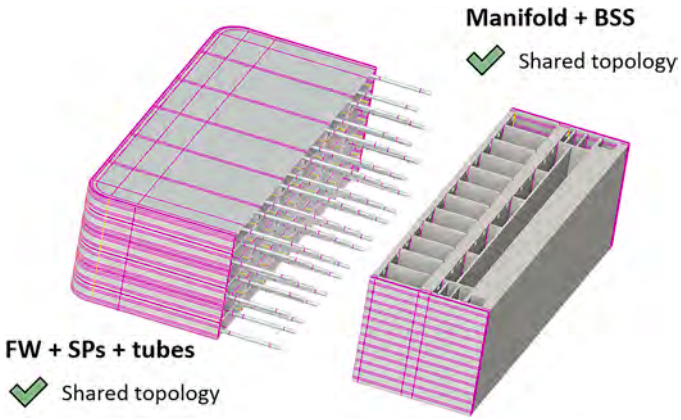

Fig. 5. Separation of the manifold and BSS from the rest of the model to keep flexibility for future design updates.

domain, initially considered for neutronic and thermal-hydraulic purposes, has been augmented to include the relevant manifold region. This expansion encompasses the appropriate sections of the water and breeder manifolds, as well as the BSS (Fig. 3). To this scope, the reference manifold and BSS geometric layout have been used since a specific manifold layout for the helical-shaped DWTs was not available yet [3]. Then, the plates of the manifold regions were properly pierced and slightly re-arranged to allow the tubes to be extruded until the corresponding inlet and outlet manifold regions. Subsequently, the resulting elementary slice was duplicated on both sides along the vertical axis to create a geometric configuration consisting of three consecutive slices (Fig. 4). Adopting this strategy, it is possible to apply mechanical restraints far enough from the region of interest (that is the BZ and the FW-SW of the central slice) to significantly reduce their impact on the results.

To maintain the geometric model's flexibility for future integration with the novel manifold architecture, the BZ and the manifold regions have been geometrically decoupled. These regions are connected in the numerical model through the implementation of appropriate contact models at their interfaces. Each of the two decoupled regions is characterized by the imposition of the "shared topology" condition, ensuring continuity of the mesh's topological features across different geometric bodies (Fig. 5). Based on this configuration, a quadratic 3D mesh comprising approximately 3.82 million nodes and connected through around 7.28 thousand hexahedral elements has been generated (Fig. 6). This mesh, along with the relevant loads and boundary conditions, has been adopted for the steady-state structural analysis to develop the FEM model.

3.2. Loading scenarios

The structural analysis of the WCLL COB segment equatorial region equipped with helical-shaped DWTs has been performed in four different load cases:

- Case 1: nominal pressure, in which the fluids (i.e. coolant and breeder) nominal pressures are assumed;
- Case 2: design pressure, in which the fluids design pressures are assumed;
- Case 3: buoyancy effect, in which the fluids design pressures and the buoyancy effect are assumed;

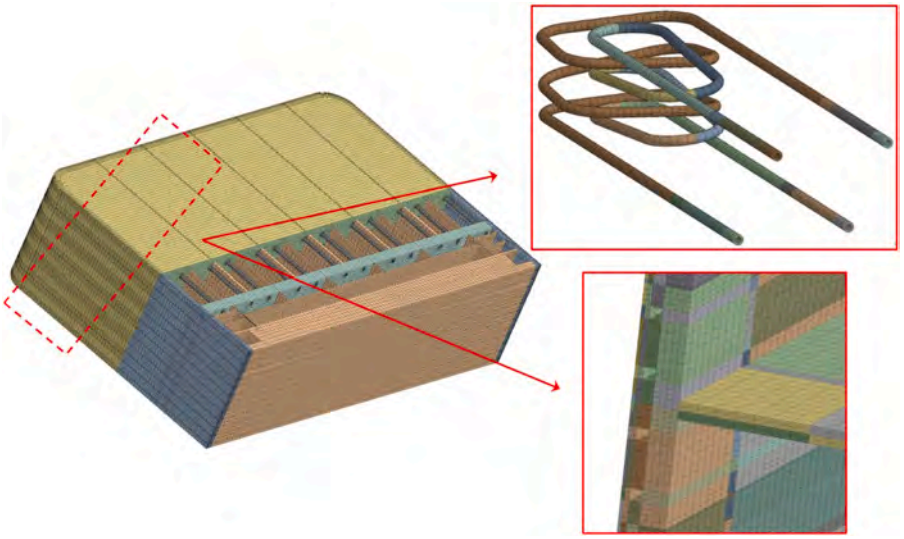

Fig. 6. Mesh of the FEM model with details in the FW and tubes.

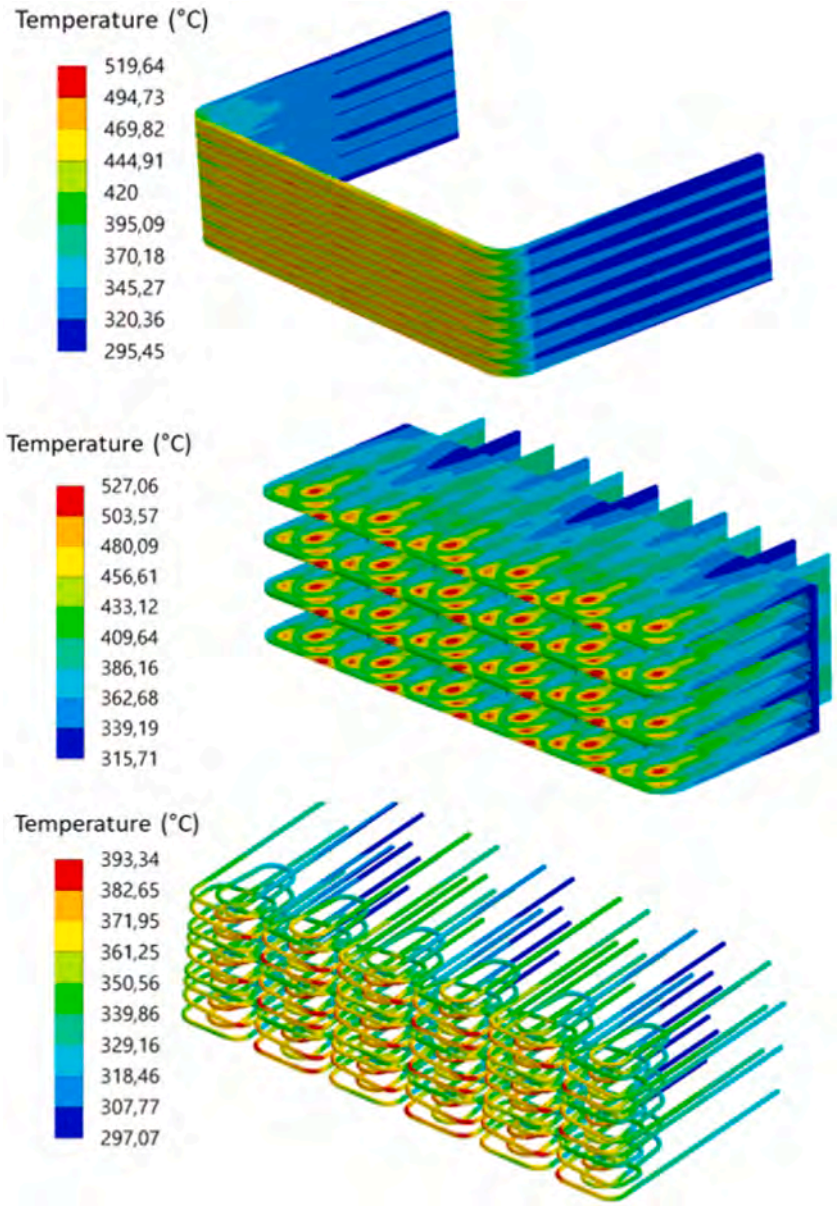

Fig. 7. Imposed thermal field condition in the FEM model in the FW (top), SPs (middle) and tubes (bottom).

- Case 4: over pressurization, in which the water design pressure is imposed on both coolant and breeder-wetted surfaces to conservatively simulate the occurrence of an in-box LOCA.

It has to be noted that no electromagnetic load has been considered in this phase of the analysis, as dedicated assessment for their determination have not been performed yet. For each case, temperature-dependent material properties have been assumed both for tungsten and Eurofer steel [16,17]. Moreover, the following loads and boundary conditions have been imposed:

- not-uniform 3D thermal strain field, calculated as the local product of the not-uniform 3D temperature distribution and the temperature-dependent volumetric expansion coefficient;
- pressure loads, depending on the considered case;
- contact models;
- mechanical restraints.

The 3D temperature distribution (Fig. 7) was calculated separately in the CFD analysis and subsequently imported into the structural FEM model as an external data set [10]. To impose a coherent thermal field on the added geometric regions (specifically the extruded tube regions and the SW in the manifold regions), it was necessary to extrapolate the temperature in the radial direction from the last mapped temperature value. Additionally, a uniform temperature of 311 °C was applied to the manifold plates and BSS, based on the results from previous studies on the reference design of the WCLL COB equatorial slice [15].

Regarding pressure loads, aimed at considering the water and breeder mechanical action, different values have been assumed on the

Table 1
Pressure loads in the analyzed cases.

Case	Water pressure [MPa]	Breeder pressure [MPa]	Buoyancy effect
1	15.5	0.5	Not considered
2	17.825	0.575	Not considered
3	17.825	0.575	Considered
4	17.825	17.825	Not considered

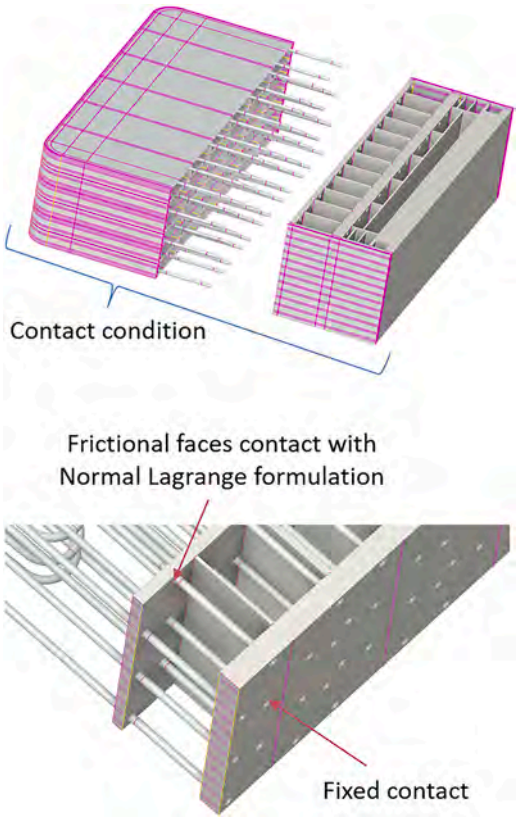

Fig. 8. Contacts among all components in the model.

basis of the considered load case [18]. They are summarised in Table 1. Regarding the breeder pressure, the static pressure value expected at the WCLL COB equatorial region has been considered.

Concerning contact models, they have been implemented to account for the mechanical interactions among the different geometric regions. A bonded contact model was first imposed at the interface between the BZ and the manifold region, treating them as perfectly tied (Fig. 8). Additionally, to address the interface between the helical-shaped DWTs and the manifolds, a bonded contact model was applied to the last back-plate (Fig. 8) to simulate the tube welding.

Instead, frictional faces contact model (characterized by a friction factor of 0.74) with Normal Lagrange formulation has been imposed in the holes of the BZ closure plate (Fig. 8). Indeed, the holes diameter (7.5 mm) is greater than the tubes external one (6.75 mm) to allow the breeder flow. During operations or accidents, the tubes and the holes may come into contact and exchange forces, which are accounted for by the imposed contact model.

As far as mechanical restraints are concerned, their scope is to reproduce the effect of the attachment system devoted to connecting the BB to the VV as well as to simulate the mechanical effect of the rest of the COB segment not included in the model. Hence, a displacement restriction condition along the vertical direction has been imposed to the nodes lying on the model's lower surface, in conjunction with a generalised plane strain condition imposed to the nodes lying on the model's upper surface. The latter condition prescribes the nodes of the considered surface to remain on the undeformed plane, which can translate along the z direction and swing with respect to the radial and toroidal axes. Lastly, the radial and toroidal displacement has been prevented to the nodes lying onto two lines obtained on the BSS external surface, as shown in Fig. 9, to allow the numerical convergence of the calculations.

4. Structural analysis and results

Adopting the FEM models described in the previous section, steady-state structural analyses have been run. The obtained results are depicted and critically discussed in this section.

4.1. Linearized stress results

Steady-state structural analyses have been conducted for all 4 load cases described previously. Generally, good behaviour in terms of Von Mises equivalent stress values has been obtained. As an example, the 3D spatial distribution of the Von Mises equivalent stress obtained in Case 1 is reported in Fig. 10. Here, only a radial-poloidal section of the assessed model is shown in order to provide details of the internals.

As it can be observed in Fig. 11, the analysis outcomes show some discontinuities in the stress results in the T-junctions in the FW and SPs. Since a shared topology condition is imposed among the different bodies composing the SPs, and in between plates and FW too, a campaign of sub-modelling analysis has been launched to investigate the local

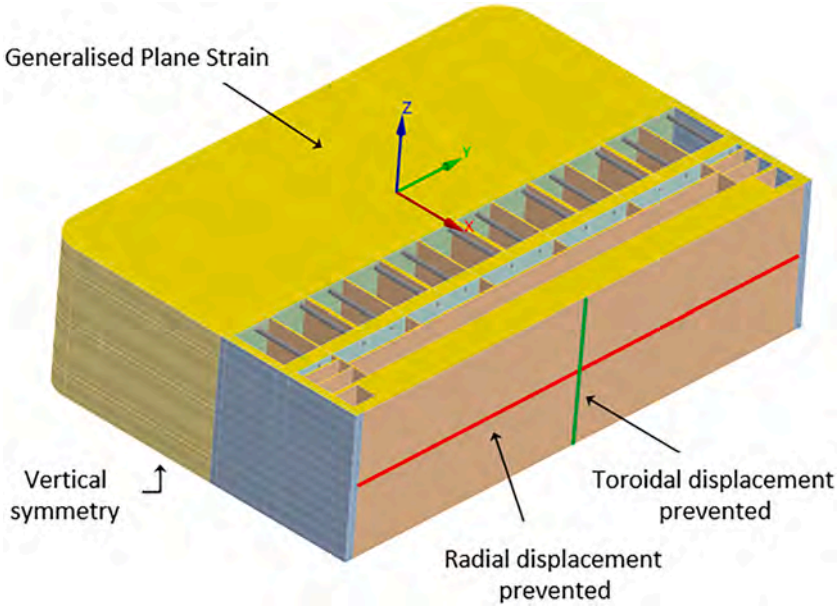

Fig. 9. Mechanical restrains in the model.

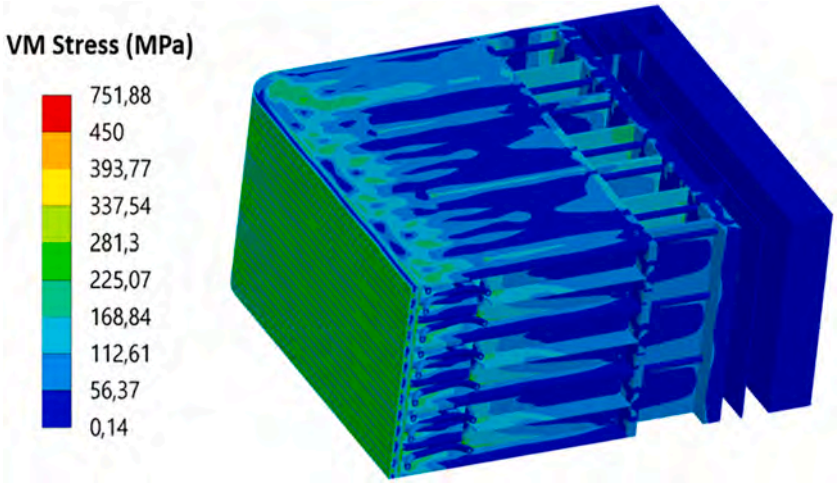

Fig. 10. Von Misses equivalent stress in the loading case 1.

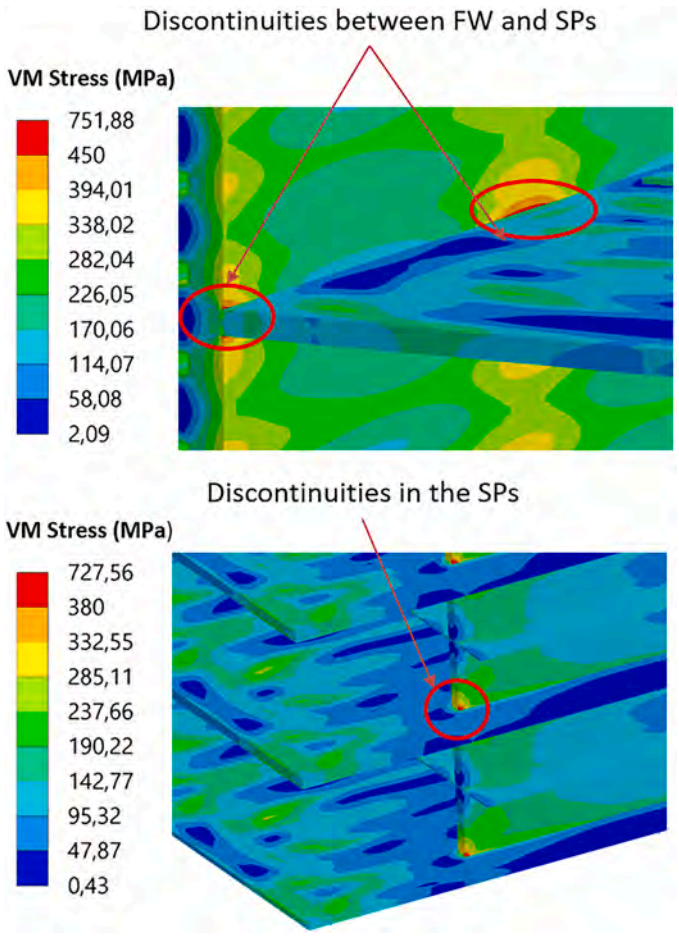

Fig. 11. Stress discontinuities in the case 1 between the FW and SPs (top) and between vertical and horizontal plates in SPs (bottom).

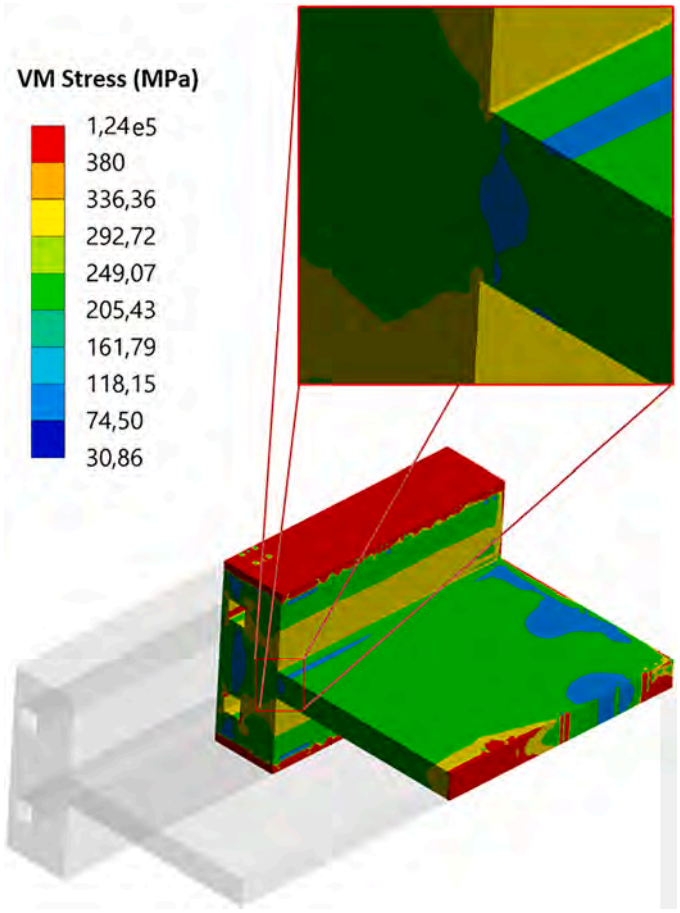

Fig. 12. Submodelling stress analysis in the FW-SPs.

behaviour of these regions. In particular, local models given by unique geometric entities have been adopted in order to exclude any influence of the adopted share topology condition, and then of the mesh settings at the interface, on the mechanical results. Hence, two sub-models have been realised: one reproducing the T-junction in between FW and SPs (Fig. 12) and the other reproducing the T-junction in between horizontal and vertical SPs (Fig. 13). The displacement obtained in the global model analysis has been mapped onto the local boundary faces and the nominal loads have been applied. Results (Figs. 12 and Fig. 13) allow finding a qualitative correspondence with the results of the global model. Hence, one can conclude that the stress discontinuities obtained in the global model are due to the system's geometric layout and to the way in which the bodies are mechanically connected. In particular, the sharp edges of the T-junctions seem to be the main responsible for such a behaviour.

In order to assess the impact of the introduced helical-shaped DWTs

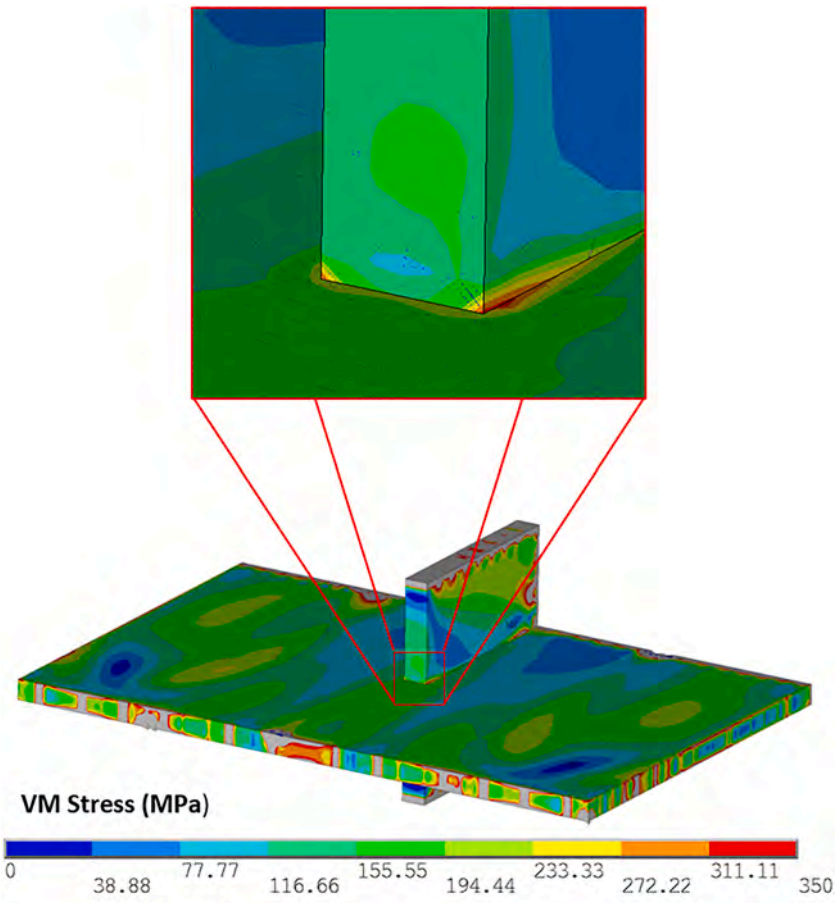

Fig. 13. Submodelling analysis in the SPs.

on the WCLL COB segment structural performances, the verification of the prescribed RCC-MRx criteria has been performed for all the 4 load cases investigated. Level A criteria have been checked for Case 1, Case 2 and Case 3 as they represent nominal load combinations whereas, as to Case 4, Level D rules have been considered since it represents a severe accident occurrence. Four criteria have been taken into account: Immediate Excessive Deformation (IED, P_m/S_m), Immediate Plastic Instability (IPI, $(P_m+P_b)/(K_{eff}\ S_m)$), Immediate Plastic Flow Localization (IPFL, $(P_m+Q_m)/S_{em}$) and Immediate Fracture due to exhaustion of ductility (IF, $(P_m+P_b+Q+F)/S_{et}$). The first two criteria only consider the primary stresses, instead the others also take into account secondary stresses occurring along the analysed path. S_m refers to the maximum allowable primary membrane stress intensity of the material, S_{em} is the maximum allowable primary plus secondary membrane stress, function of temperature and irradiation, S_{et} is the maximum allowable total stress, also function of temperature and irradiation, and, finally, K_{eff} is a factor called "plastic collaboration coefficient", equal to 1.5 for rectangular sections.

For each criterion, the stress limit values have been calculated, for the service level to which each loading scenario analysed relates, in accordance with the structural material and the average path temperature (T_{ave}). The selection of the most critical zones for the paths constructions has been driven by the values of the ratio between the Von Mises stress and the temperature-dependent stress limit S_m. The user-defined field given by the ratio of these two quantities, calculated invoking the nodal temperature, has been created and the paths have been built throughout those areas where the ratio is considerably greater than one. The attention has been paid to the central slice, as it is the farthest from the model's boundaries. Since the assessed load cases differ only for the applied pressure loads, differences in the Von Mises stress over S_m ratio are only due to the considered pressure loads and, specifically, are due to the variation in the Von Mises stress originated by the different pressure loads set. Hence, its representation is a straightforward measure of the stress level achieved within the structure in each load case.

As to Case 1 results, the Von Mises stress over S_m field calculated within FW-SW and SPs of the central slice is shown in Fig. 14. Here, the path locations are highlighted. Despite the fact that in large areas the Von Mises stress fields exceed the S_m value, the prescribed RCC-MRx criteria are largely fulfilled as reported in Table 2. Even the IPFL criterion, which normally achieves high values in the WCLL BB structural analysis, is satisfied with a remarkable margin. As to the helical-shaped DWTs, the resulting Von Mises stress over S_m field is shown in Fig. 15. Since values considerably lower than 1 are predicted, no criteria verification is necessary as the predicted structural response can be judged safe.

As to Case 2 and Case 3, very close results are obtained both in terms of Von Mises stress field and criteria verification. Indeed, the pressure increase in Case 2 (where the design pressures are considered instead of the nominal ones) and the activation of the buoyancy forces (in Case 3) do not have a remarkable impact on the stress amount prediction, as well as on its distribution. This result could have been predicted considering that, typically, the most intense contribution is given by the secondary stress that remains unchanged among the 3 cases whereas slight variations of the pressure loads are assumed.

Instead, as regards Case 4, the Von Mises stress over S_m field calculated within FW-SW and SPs of the central slice is shown in Fig. 16. Differently from the nominal conditions, under accidental load combinations the sidewalls are quite loaded and therefore the fulfilment of the RCC-MRx criteria has to be checked also there. Even in the SPs domain,

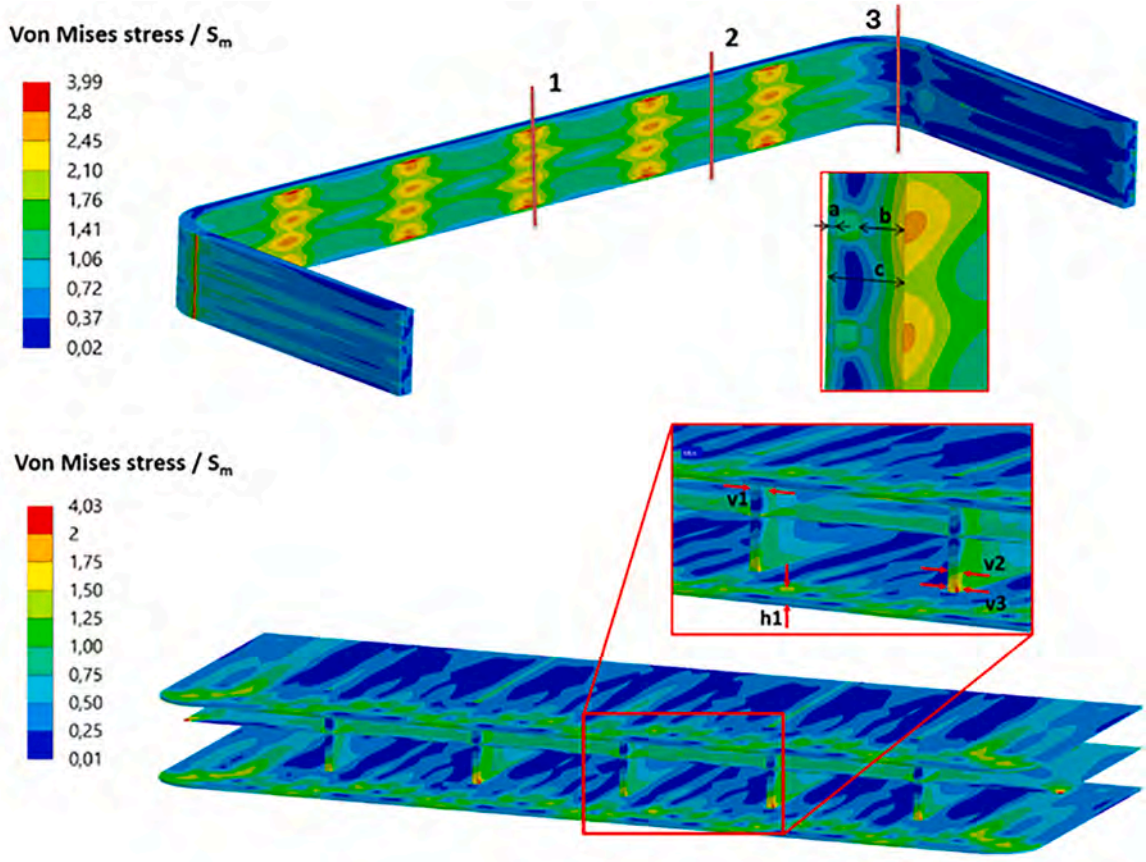

Fig. 14. Case 1 - Von Mises stress over S_m field within FW-SW and SPs of the central slice.

Table 2
Case 1 – RCC-MRx Level A criteria verification.

Path	T_{ave} [°C]	P_m/S_m	$(P_m+P_b)/(K_{eff} \bullet S_m)$	$(P_m+Q_m)/S_{em}$	$(P_m+P_b+Q+F)/S_{et}$
FW_1a	390.7	0.09	0.53	0.16	0.12
FW_1b	441.9	0.10	0.63	0.20	0.13
FW_1c	480.4	0.09	0.41	0.14	0.07
FW_2a	373.0	0.02	0.15	0.10	0.03
FW_2b	392.0	0.08	0.21	0.09	0.10
FW_2c	404.8	0.07	0.31	0.12	0.06
FW_3a	378.9	0.02	0.39	0.14	0.01
FW_3b	409.5	0.09	0.36	0.14	0.13
FW_3c	446.8	0.09	0.29	0.11	0.06
SP_v1	445.6	0.02	0.01	0.41	0.07
SP_v2	417.3	0.03	0.02	0.62	0.12
SP_v3	392.4	0.13	0.13	0.59	0.15
SP_h1	442.6	0.03	0.02	0.18	0.03

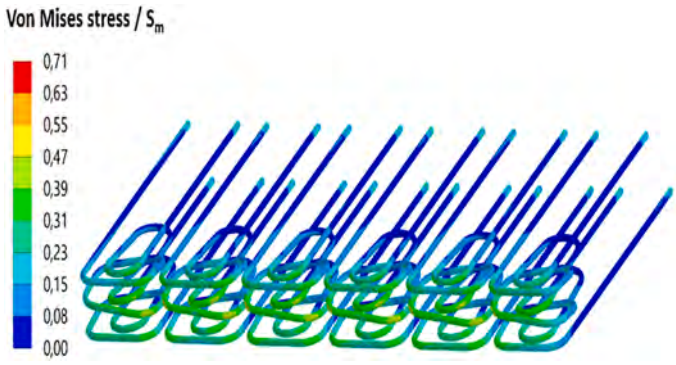

Fig. 15. Case 1 - Von Mises stress over S_m field within the helical-shaped tubes of the central slice.

the stress amount is remarkable and additional paths are necessary to assess its structural response in view of the RCC-MRx code. Hence, the obtained results are reported in Table 3. It has to be noted that Level D stress limits have been used for this case.

Globally, a very good behaviour can be predicted even under accidental conditions represented by the Case 4, since the criteria are not fulfilled only along a few paths and in any case with a very small margin. Even the stress arising within the helical-shaped DWTs is greater than in the nominal cases (Fig. 17), but the highest values are calculated in correspondence with the bonded contact with the manifold plates. In the rest of the DWTs domain, quite low values of the Von Mises stress over S_m ratio (< 0.6) are still obtained notwithstanding the accidental conditions, suggesting that no criteria verification is necessary to prove the safe DWTs structural behaviour.

4.2. Displacement field

Besides the stress evaluation, the relative displacements between adjacent helical-shaped tubes and between a tube and the closest plate have been checked. This analysis has been performed only under nominal conditions (namely in Case 1, Case 2 and Case 3) since under the accidental scenario (Case 4) the replacement of the component is necessary reagardless of any tubes hits the SB.

As to Case 1 and Case 2, quite similar results in terms of relative displacement have been obtained. Since variations of the order of the tens of microns are calculated, the results have been assumed being the same. In particular, the displacement fields along x, y and z directions have been checked and the nodal relative displacement has been calculated to check if adjacent tubes hit each other and if tubes hit the

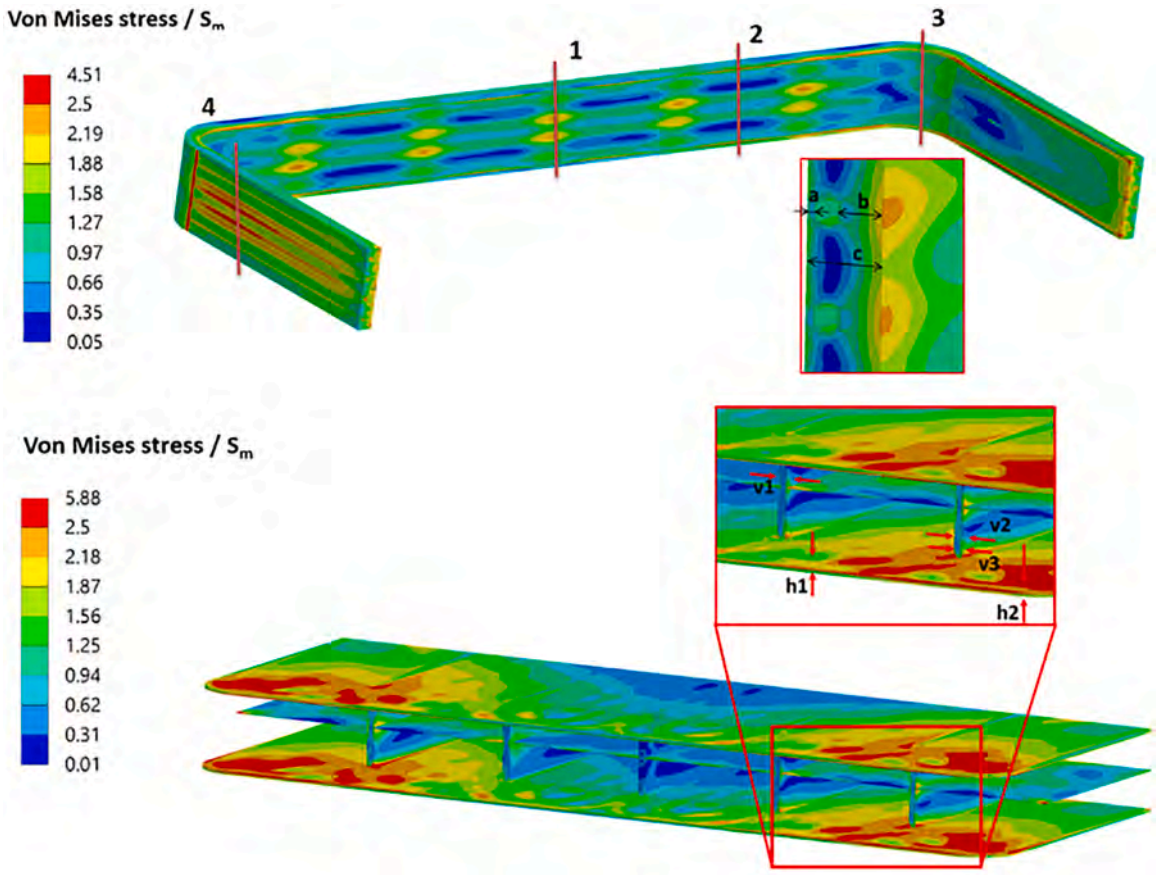

Fig. 16. Case 4 - Von Mises stress over S_m field within FW-SW and SPs of the central slice.

Table 3
Case 4 – RCC-MRx Level D criteria verification.

Path	T_{ave} [°C]	P_m/S_m	$(P_m+P_b)/(K_{eff}\bullet S_m)$	$(P_m+Q_m)/S_{em}$	$(P_m+P_b+Q+F)/S_{et}$
FW_1a	390.7	1.06	0.78	0.71	0.23
FW_1b	441.9	1.14	0.84	0.45	0.18
FW_1c	480.4	0.85	0.71	0.25	0.06
FW_2a	373	0.70	0.47	0.23	0.08
FW_2b	392	0.36	0.29	0.23	0.10
FW_2c	404.8	0.50	0.46	0.20	0.09
FW_3a	378.9	0.29	0.46	0.57	0.22
FW_3b	409.5	0.92	0.69	0.29	0.19
FW_3c	446.8	0.62	0.56	0.16	0.04
FW_4a	328.7	0.35	0.49	1.09	0.41
FW_4b	350	0.97	0.79	0.38	0.26
FW_4c	343.6	0.42	0.44	0.40	0.31
SP_v1	445.6	0.59	0.43	0.09	0.02
SP_v2	417.3	0.32	0.21	0.20	0.05
SP_v3	392.4	0.00	0.00	0.27	0.13
SP_h1	442.6	0.36	0.31	0.48	0.09
SP_h2	466.8	0.50	0.46	1.02	0.17

close stiffening plate or FW-SW. The most critical regions have resulted being those circled in Fig. 18.

For each region, the attention has been paid to the closest nodes in terms of residual relative distance along a given direction, calculated and compared with the initial one. The results are summarized in Table 4. As it can be observed, the tubes do not hit FW and SW (locations 1, 2 and 3). Actually, the relative distance increases because of the different expansion on the X-Y plane of DWTs and segment box. On the contrary, the tubes move closer to the SPs and to the baffle plate along the vertical direction. The most critical situation is that found in location 5, where two DWTs move closer along the Z direction with a very small residual gap of only 0.8 mm. Globally, a good behaviour of the helical-shaped DWTs can be predicted also in terms of relative displacement even if a narrow residual gap is predicted in some cases.

As to Case 3, results of the same kind can be obtained (here not reported for the sake of brevity). In particular, it has been found that considering the buoyancy forces does not produce contact in between the tubes or between tubes and plates along the vertical direction. Also in this case, some narrow residual gaps along the vertical direction are found between some tubes but no contact is predicted.

Lastly, the potential onset of contacts in the holes of the BZ closure plate has been checked under nominal conditions. Again, in case of accident the main issue is definitely not represented by the possible contact between a tube and the hole.

As to Case 1 and Case 2, results are shown in Fig. 19. As it can be observed, contact between tubes and holes only occurs in one location. The contact pressure is also reported (Fig. 20), observing that the contact area is quite small and that, in Case 1, the contact mode is sticking whereas in Case 2 a sliding contact takes place.

Instead, concerning Case 3, no contact is predicted at all even though a very small residual gap (< 0.5 mm) is calculated. This could pose problems for the lead lithium circulation, suggesting to carefully review the holes diameter.

5. Conclusions

In conclusion, the structural analysis of the equatorial region of the WCLL COB segment equipped with helical-shaped tubes has predicted a very promising behaviour in terms of RCC-MRx criteria verification. Under normal operating conditions, the helical-shaped DWTs demonstrated excellent structural performance, easily meeting the prescribed

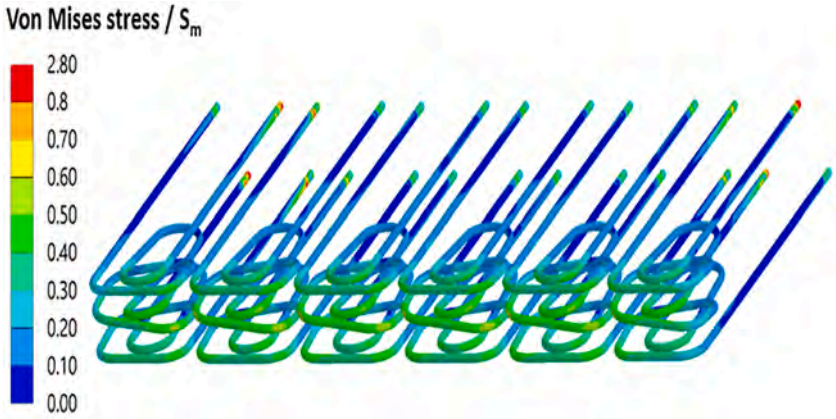

Fig. 17. Case 4 - Von Mises stress over S_m field within the helical-shaped tubes of the central slice.

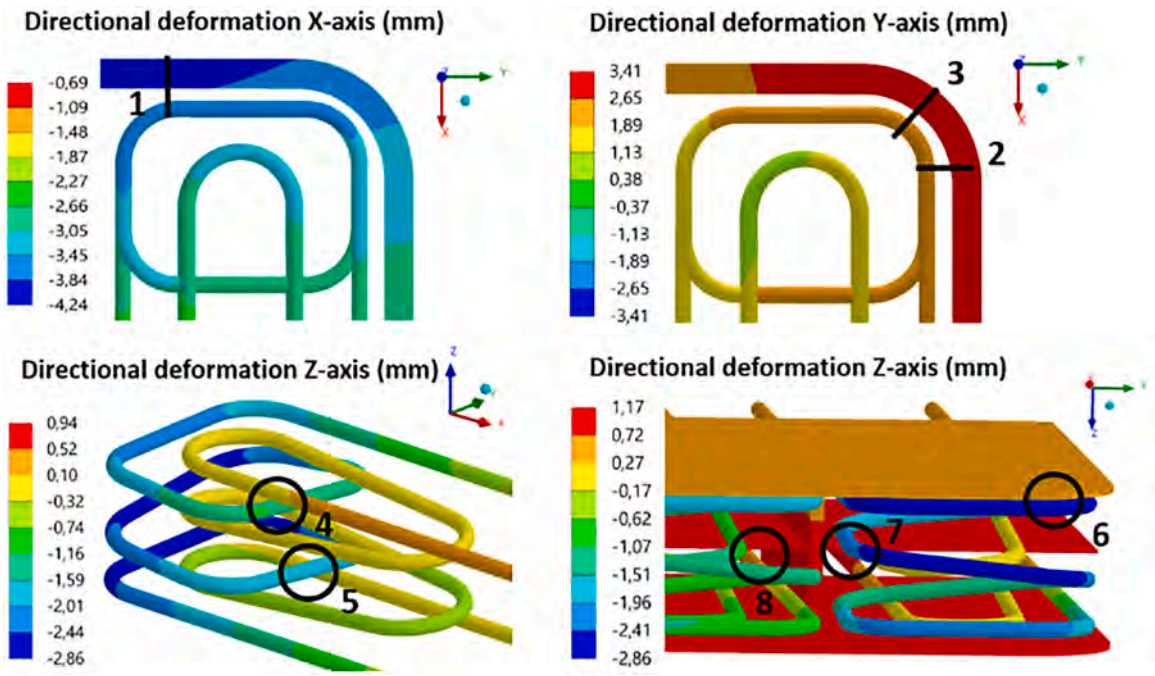

Fig. 18. Case 1 and 2 - Directional displacements.

Table 4
Case 1 and Case 2 – Relative distances.

Interfacing components		Ref. Fig. 18		Relative distance [mm]	
		Number	*Direction*	Initial	*Deformed*
FW	Tube	1	X	10.0	10.0
FW	Tube	2	Y	13.8	14.5
FW	Tube	3	X, Y	8.0	9.2
Tube	Tube	4	Z	1.8	3.1
Tube	Tube	5	Z	2.4	0.8
Tube	SP	6	Z	5.8	2.4
Tube	Baffle Plate	7	Z	6.4	5.5
Tube	SP	8	Y	1.9	1.9

safety criteria with a substantial margin. This indicates that the helical design is robust and well-suited for standard operational loads. Although some areas showed higher stress under accidental loading conditions, these stresses were still within acceptable limits.

The analysis of displacements revealed narrow gaps between adjacent DWTs and between the tubes and structural plates. However, there was no actual contact predicted under nominal conditions, and even under accidental scenarios, the integrity of the tubes was maintained, indicating that the design can tolerate significant loads without critical deformation. The helical-shaped DWTs displayed a favourable stress distribution with lower Von Mises stress values compared to the traditional C-shaped configuration. This suggests improved mechanical performance and reliability, reinforcing the viability of the helical design for the WCLL BB.

CRediT authorship contribution statement

J.A. Noguerón: Writing – original draft, Visualization, Validation, Software, Investigation, Formal analysis. **P.A. Di Maio:** Supervision, Project administration, Methodology, Funding acquisition, Conceptualization. **G. Bongiovì:** Writing – review & editing, Methodology, Formal analysis, Data curation, Conceptualization. **I. Catanzaro:** Writing – review & editing, Methodology, Formal analysis, Conceptualization. **P. Chiovaro:** Supervision, Methodology, Conceptualization. **S. Giambrone:** Visualization, Software, Methodology, Investigation. **A. Quartararo:** Writing – review & editing, Software, Methodology,

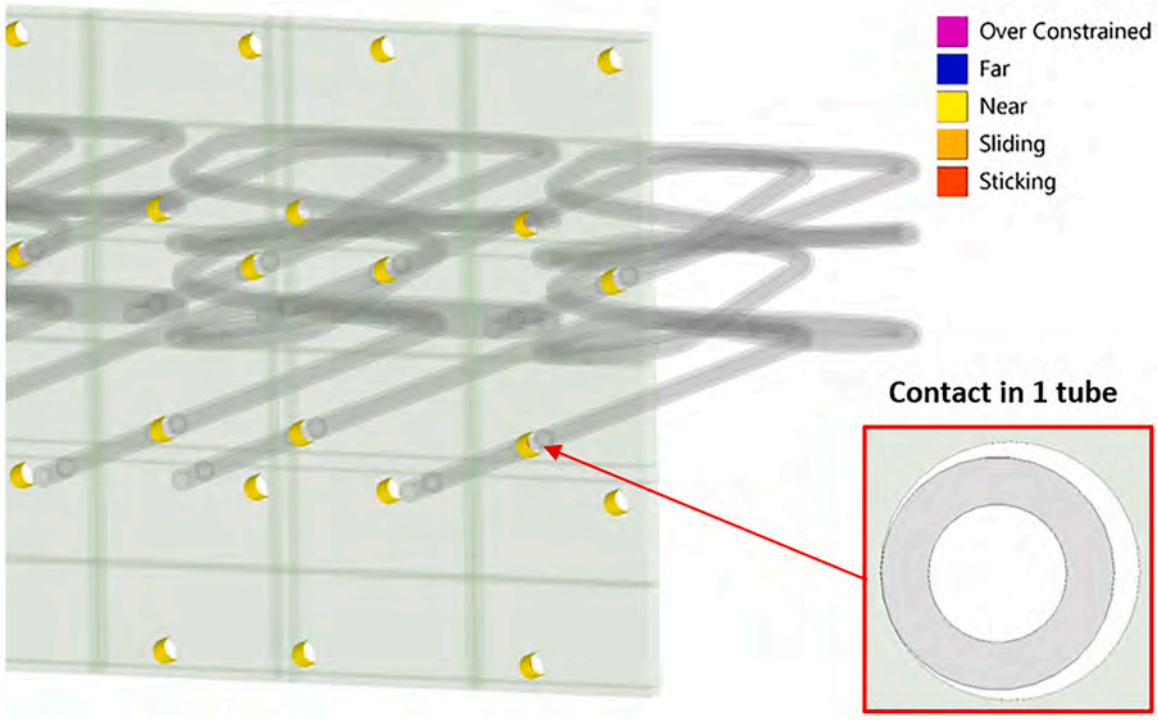

Fig. 19. Contacts in between holes and tubes.

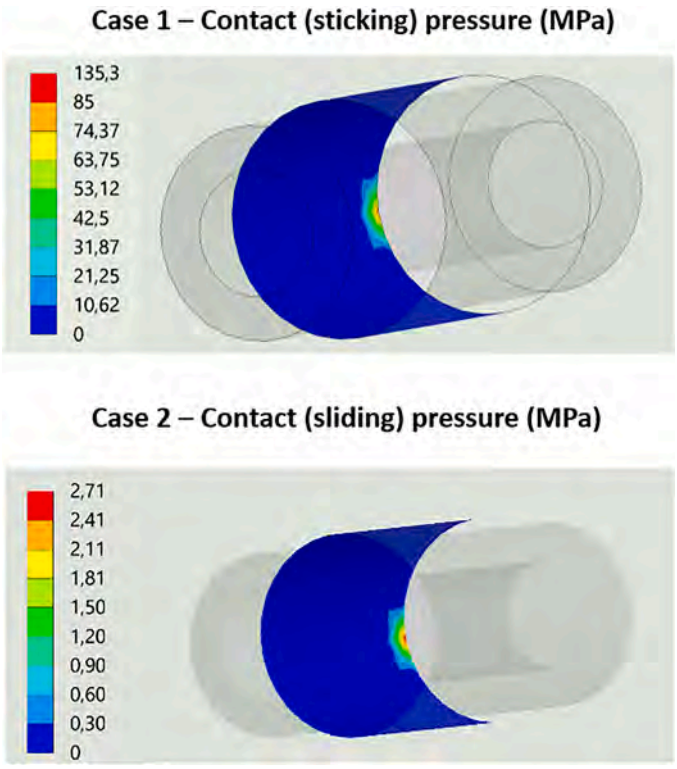

Fig. 20. Pressure analysis of contacts between tubes and holes in cases 1 (top) and 2 (bottom).

Conceptualization. **E. Vallone:** Supervision, Methodology, Conceptualization. **I. Fernández-Berceruelo:** Writing – review & editing, Supervision, Software, Resources. **P. Arena:** Supervision, Resources, Project administration, Formal analysis.

Declaration of competing interest

The authors declare that they have no known competing financial interests or personal relationships that could have appeared to influence the work reported in this paper.

Acknowledgements

This work has been carried out within the framework of the EUROfusion Consortium, funded by the European Union via the Euratom Research and Training Programme (Grant Agreement No 101052200 —EUROfusion). Views and opinions expressed are however those of the author(s) only and do not necessarily reflect those of the European Union or the European Commission. Neither the European Union nor the European Commission can be held responsible for them.

This work has been partially supported by the ENEN2plus project (HORIZON-EURATOM-2021-NRT-01–13 101061677) founded by the European Union.

Data availability

Data will be made available on request.

References

[1] G. Federici, C. Bachmann, L. Barucca, C. Baylard, W. Biel, L.V. Boccaccini, J. H. You, Overview of the DEMO staged design approach in Europe, Nucl. Fusion 59 (6) (2019) 066013, https://doi.org/10.1088/1741-4326/ab1178.

[2] F.A. Hernández, P. Pereslavtsev, G. Zhou, Q. Kang, S. D'Amico, H. Neuberger, F. Cismondi, Consolidated design of the HCPB breeding blanket for the preconceptual design phase of the EU DEMO and harmonization with the ITER HCPB TBM program, Fusion Eng. Des. 157 (2020) 111614, https://doi.org/10.1016/j.fusengdes.2020.111614.

[3] P. Arena, et al., The DEMO water-cooled lead–lithium breeding blanket: design status at the end of the pre-conceptual design phase, App. Sci. 11 (2021) 11592, https://doi.org/10.3390/app112411592.

[4] P. Arena, et al., Design and integration of the EU-DEMO water-cooled lead lithium breeding blanket, Energies 16 (2023) 2069, https://doi.org/10.3390/en16042069.

[5] E. Martelli, A. Del Nevo, P. Arena, G. Bongiovì, G. Caruso, P.A. Di Maio, M. Eboli, G. Mariano, R. Marinari, F. Moro, et al., Advancements in DEMO WCLL breeding

blanket design and integration, Int. J. Energy Res. 42 (2018) 27–52, https://doi.org/10.1002/er.3750.
[6] A. Tassone, A. Del Nevo, P. Arena, G. Bongiovì, G. Caruso, P.A. Di Maio, G. di Gironimo, M. Eboli, N. Forgione, R. Forte, et al., Recent progress in the WCLL breeding blanket design for the DEMO fusion reactor, IEEE Trans. Plasma Sci. 46 (2018) 1446–1457, https://doi.org/10.1109/TPS.2017.2786046/.
[7] G. Pintsuk, E. Diegele, S. Dudarev, et al., European materials development: results and perspective, Fusion Eng. Des. 146 (2019) 1300–1307, https://doi.org/10.1016/j.fusengdes.2019.02.063.
[8] D. Martelli, A. Venturini, M. Utili, Literature review of lead-lithium thermophysical properties, Fusion Eng. And Des. 138 (2019) 183–195, https://doi.org/10.1016/j.fusengdes.2018.11.028.
[9] L.V. Boccaccini, et al., Status of maturation of critical technologies and systems design: breeding blanket, Fusion Eng. Des 179 (2022) 113116, https://doi.org/10.1016/j.fusengdes.2022.113116.
[10] P. Maccari, P. Arena, R. Marinari, A. Del Nevo, F. Moro, S. Noce, Helical-shaped double wall tubes solution for the breeding zone cooling in the WCLL breeding blanket, Fusion Eng. Des. 199 (2024) 114134, https://doi.org/10.1016/j.fusengdes.2023.114134.
[11] C. Bachmann, S. Ciattaglia, F. Cismondi, T. Eade, G. Federici, U. Fischer, T. Franke, C. Gliss, F. Hernandez, J. Keep, et al., Overview over DEMO design integration challenges and their impact on component design concepts, Fusion Eng. Des. 136 (2018) 87–95, https://doi.org/10.1016/j.fusengdes.2017.12.040.
[12] F. Edemetti, I. Di Piazza, A. Del Nevo, G. Caruso, Thermal-hydraulic analysis of the DEMO WCLL elementary cell: BZ tubes layout optimization, Fusion Eng. Des. 160 (2020) 111956, https://doi.org/10.1016/j.fusengdes.2020.111956.
[13] A. Tassone, G. Caruso, F. Giannetti, A. Del Nevo, MHD mixed convection flow in the WCLL: heat transfer analysis and cooling system optimization, Fusion Eng. Des. 146 (2019) 809–813, https://doi.org/10.1016/j.fusengdes.2019.01.087.
[14] U. Fischer, et al., Required, achievable and target TBR for the European DEMO, Fusion Eng. Des. 155 (2020) 111553, https://doi.org/10.1016/j.fusengdes.2020.111553.
[15] I. Catanzaro, et al., Analysis of the thermo-mechanical behaviour of the EU DEMO water-cooled lithium lead central outboard blanket segment under an optimized thermal field, Appl. Sci. 12 (3) (2022) 1356, https://doi.org/10.3390/app12031356.
[16] E. Gaganidze, Material Properties Handbook – EUROFER97 (2023), IDM Ref.: eFDA_D_2NZHBS.
[17] E. Gaganidze, F. Schoofs, Material Properties Handbook – Tungsten (2020), IDM Ref.: eFDA_D_2P3SPL.
[18] G.A. Spagnuolo, et al., Development of load specifications for the design of the breeding blanket system, Fusion Eng. Des. 157 (2020) 11657, https://doi.org/10.1016/j.fusengdes.2020.111657.